Synthesis and Splice-Redirecting Activity of Branched, Arginine-Rich Peptide Dendrimer Conjugates of Peptide Nucleic Acid Oligonucleotides

Amer F. Saleh,[†] Andrey Arzumanov,[†] Rachida Abes,[§] David Owen,[†] Bernard Lebleu,[§] and Michael J. Gait*,[†]

Medical Research Council, Laboratory of Molecular Biology, Hills Road, Cambridge, CB2 0QH, United Kingdom, and UMR 5235 CNRS, Université Montpellier 2, Place Eugene Bataillon, 34095 Montpellier cedex 5, France. Received June 17, 2010; Revised Manuscript Received September 7, 2010

Arginine-rich cell-penetrating peptides have found excellent utility in cell and in vivo models for enhancement of delivery of attached charge-neutral PNA or PMO oligonucleotides. We report the synthesis of dendrimeric peptides containing 2- or 4-branched arms each having one or more R-Ahx-R motifs and their disulfide conjugation to a PNA705 splice-redirecting oligonucleotide. Conjugates were assayed in a HeLa pLuc705 cell assay for luciferase up-regulation and splicing redirection. Whereas 8-Arg branched peptide−PNA conjugates showed poor activity compared to a linear $(R\text{-Ahx-R})_4$−PNA conjugate, 2-branched and some 4-branched 12 and 16 Arg peptide−PNA conjugates showed activity similar to that of the corresponding linear peptide−PNA conjugates. Many of the 12- and 16-Arg conjugates retained significant activity in the presence of serum. Evidence showed that biological activity in HeLa pLuc705 cells of the PNA conjugates of branched and linear (R-Ahx-R) peptides is associated with an energy-dependent uptake pathway, predominantly clathrin-dependent, but also with some caveolae dependence.

INTRODUCTION

Cell-penetrating peptides (CPPs) have proven extremely valuable for enhancing the cell delivery of a range of biomolecules either as covalent conjugates or as noncovalent complexing agents (*1*). Among the biocargoes that are well-suited for CPP conjugation are antisense oligonucleotide (ON) analogues that are used to target RNAs inside cells (*2, 3*). Particularly good results have been obtained in cell delivery when CPPs are conjugated to charge-neutral peptide nucleic acid (PNA) and phosphorodiamidate morpholino oligonucleotides (PMO) that are used for non-RNase-H steric block antisense applications (*4, 5*). Such ON analogues are metabolically stable inside cells and in tissues, and retain very good sequence specificity in binding to RNA targets. Peptide conjugates of PNA and PMO are now being investigated in therapeutic applications, for example, for redirecting RNA splicing in diseases such as Duchenne muscular dystrophy (DMD) (*6, 7*).

A wide range of CPPs has been proposed for PNA and PMO conjugation, some of which are derived from small transduction domains of proteins (Tat (48−60), Penetratin), and many others are composite or synthetically designed (*2, 3*). Most CPPs are cationic, and often, they also contain regions of hydrophobic amino acids. Cationic charge helps the binding of the CPP to the cell surface glycosaminoglycans. However, the mechanisms of cell uptake following cell surface binding are diverse and in some cases have proven controversial. It is commonly recognized that in most cases at modest concentrations (1 μM or less) and, especially when conjugated to an ON cargo, endocytotic uptake mechanisms of CPPs predominate, rather than direct translocation (*2, 3*). Cationic and hydrophobic elements in the CPP are also thought to help to enhance their release from endosomes into the cytosol, but the exact spatial parameters for optimal release are not well understood.

* Corresponding author. Michael J. Gait, Tel: +44 1223 402473; fax: +44 1223 420270; E-mail: mgait@mrc-lmb.cam.ac.uk.

[†] Medical Research Council, Laboratory of Molecular Biology.

[§] UMR 5235 CNRS.

It has become well accepted that when viewed by live-cell confocal microscopy fluorescently tagged cationic CPP-ON conjugates usually become sequestered within endosomal compartments (*8*). However, to interact with mRNA or pre-mRNA targets, ONs must reach the cytosol or nucleus, respectively. In order to better understand what parameters within an attached CPP are required to help endosomal release and thus allow the attached ON to reach its RNA target, it is necessary to utilize a biological assay that is characteristic of the cell compartment. Kole and colleagues developed such an assay for the nucleus, whereby HeLa cells contain an integrated pLuc705 plasmid coding for a firefly luciferase gene within which is embedded an aberrant β-globin intron. To produce firefly luciferase, it is necessary to deliver into the nucleus of the HeLa cells an 18-mer synthetic ON (which is targeted to the 705 site) to restore correct splicing of the pre-mRNA and hence a functional luciferase mRNA (*9*). This assay is straightforward and has a high dynamic range, which allows both high and low activity levels to be measured quantitatively as a positive luminescence readout. In addition, the EC_{50} of the splicing redirection can be assessed readily at the RNA level by an RT-PCR assay.

By use of the HeLa pLuc705 assay, we have reported that Arg-rich peptides are particularly valuable as delivery agents into cells when covalently conjugated to PNA or PMO ON cargoes in the absence of any transfection or other delivery agent. For example, we found that $(R\text{-Ahx-R})_4$-PNA705 and $(R\text{-Ahx-R})_4$-PMO705 conjugates (Ahx = aminohexanoic acid) were able to redirect splicing more efficiently than conjugates of Tat, Penetratin, or oligo-Arg classical CPPs (*10*−*12*). The interspersing of the non-natural Ahx amino acids is advantageous in providing an optimal spatial distribution of guanidinium side chains, in increasing metabolic stability, and in decreasing cytotoxicity (*13, 14*).

Further, the active fraction of such conjugates appears to enter HeLa pLuc705 cells predominantly by energy-dependent endocytosis (*10*), similarly to that found previously for PNA conjugates of Tat peptide (*15*). In addition, Arg-rich conjugates of

10.1021/bc100275r
Published on Web 09/29/2010

PMO ONs have been shown to be highly effective in enhancing muscle cell delivery and exon skipping in a *mdx* mouse model of Duchenne muscular dystrophy (DMD), and such conjugates are in preclinical development (*6*). Other candidate Arg-rich peptides (such as Pip peptides and B-MSP) also utilize R-Ahx-R or R-β-R (β = beta-alanyl) motifs and have been used successfully to deliver PMO with even higher activity in *mdx* mice (*16, 17*).

We described recently a synthetic, Arg-rich tetramerizing peptide R10p53^{tet} where ten Arg residues were added to the *N*-terminus of the well-defined tetramerization domain of p53 protein (*18*). The peptide was conjugated close to its C-terminus to the PNA705 18-mer used in splice-redirecting studies. The splicing redirection efficiency of the PNA705 when added to HeLa pLuc705 cells was found to be much greater for the R10p53^{tet} conjugate than for R10p53^{mono}, a point mutant in the p53 domain that had been shown previously to be unable to tetramerize. The R10p53^{tet}-PNA705 conjugate was more active than any of the conjugates to CPPs previously tested by us in this assay, such as Tat (*12, 19*), Penetratin (*19*), R_6-Penetratin (*19*), and Pip2b (*16*). However, the R10p53^{tet} peptide was long (50 amino acids) and the synthetic yields were not high, and therefore, this paradigm does not seem likely to be readily adaptable for in vivo studies. Nevertheless, the principle of multivalency seemed to be highly beneficial as originally suggested (*20*).

Several years ago, Futaki and colleagues reported branched-chain arginine peptides where 4 or 8 short oligo-Arg chains were constructed based on chain branching through both the α and ε positions of Lys residues (*21*). The best translocation into HeLa cells was observed when the Arg residues were interspersed with three Gly residues (RG_3R) and placed on a four-armed structure, resulting in a branched 8-arginine configuration. This branched peptide was conjugated either directly to fluorescein or to the protein carbonic anhydrase labeled with fluorescein, and the translocation was visualized by confocal microscopy. Unfortunately, at that time confocal microscopy was carried out in the presence of a cell fixative (acetone/methanol), conditions now known to result in artifactual cell uptake and intracellular redistribution of cationic peptides (*8*). More recently, 4-branched RG_3R peptides with an Alexa fluorescent dye attached were shown to locate in endosomal compartments using live-cell imaging (*22*). However, no activity data for any attached cargo were reported.

Another recent development has been the use of a synthetic dendrimer where eight guanidine moieties were arranged to branch from a central triazine core by means of hexyl spacers (*23*). When attached to PMO oligonucleotides, the octa-guanidino dendrimer was able to enhance cell delivery of the PMO in cultured cells in the presence of serum and also enhance delivery in vivo in a wide range of tissues (*23, 24*). These conjugates are sold commercially as "Vivo-morpholinos". Thus, the concept of spacing arginine (or guanidine) moieties in a three-dimensional dendrimer configuration seemed worth exploring further.

We now describe straightforward solid-phase techniques for the chemical synthesis of 2- and 4-branched Arg-rich peptide dendrimers where such branches contain multiple (R-Ahx-R) motifs. Such branched peptides were conjugated to a charge-neutral PNA705 cargo and evaluated for their splice-redirecting activity in a HeLa pLuc705 system in comparison to equivalent linear peptides. Whereas 8-Arg branched peptide−PNA conjugates showed poor activity compared to linear peptide−PNA conjugate, 2-branched and some 4-branched 12 and 16 Arg peptide−PNA conjugates showed activities similar to those of the corresponding linear peptide−PNA conjugates. Many of the 12- and 16-Arg conjugates retained significant activity in the presence of serum. Evidence was shown that biological activity of the peptide−PNA in HeLa cells is associated primarily with an energy-dependent uptake pathway, predominantly clathrin-dependent, but that caveolae can also play a role.

EXPERIMENTAL PROCEDURES

Synthesis of Linear and Branched (R-Ahx-R)-Containing Peptides. Peptide syntheses were carried out using a CEM Liberty microwave peptide synthesizer by Fmoc chemistry. Linear peptides were synthesized starting with 100 μmol of functionalized Fmoc-PAL-PEG-PS solid support (Applied Biosystems), 2-branched peptides were synthesized starting with 50 μmol of support, and 4-branched peptides starting with 25 μmol of support. For all branched peptide syntheses, each Fmoc amino acid derivative was made up to the same concentration as if it was a standard 100 μmol-scale linear synthesis. Thus, for a 2-branched peptide, the excess activated Fmoc amino acid over growing chains in the coupling reactions after the chain branching step was 10-fold, and for a 4-branch peptide, the excess after two branching steps was 5-fold. Coupling reactions were carried out using Fmoc-amino acids in DMF activated with 0.99 equiv of PyBop in DMF and 1.98 equiv of diisopropylethylamine (DIPEA) in *N*-methylpyrrolidone (NMP). The branch point amino acid derivative was Fmoc-Lys(Fmoc)−OH (Novabiochem). Fmoc-Arg(Pbf)−OH (Novabiochem) was used for Arg couplings with the microwave double-coupling protocol previously reported (*25*). Fmoc-deprotection at each cycle was carried out using 20% piperidine in DMF containing 0.1 M hydroxybenzotriazole (HOBT). The final peptidyl resin was washed with DMF and then dichloromethane and dried in vacuo.

Cleavage and deprotection were carried out using TFA/water/ethanedithiol/triethylsilane (94:2.5:2.5:1, 20 mL) for 2 h, the resin removed by filtration and washed with TFA (ca. 5 mL) and the filtrate sparged with nitrogen to obtain a small volume. The peptide was precipitated by addition of cold diethyl ether, collected by centrifugation, and the pellet washed a further 5 times with cold ether (25 mL).

Preparative HPLC was carried out using a Phenomenex Jupiter 10 μ C18 column (250 × 10 mm): buffer A, 0.1% TFA in water; buffer B, acetonitrile containing 10% buffer A. Elution was with a linear gradient of 15−50% buffer B over 25 min. Detection was at 215/230 nm (diode array) with a flow rate of 3.5 mL min^{-1}. Analytical HPLC used the same column type (5 μ, 250 × 4.6 mm) and similar buffer and 10−40% B over 25 min gradient conditions (1.5 mL min^{-1}). Representative HPLC traces for branched peptides are shown in Supporting Information Figure 1. MALDI-TOF mass spectral analysis used a Voyager DE Pro BioSpectrometry workstation with a matrix of α-cyano-4-hydroxycinnamic acid, 10 mg mL^{-1} in acetonitrile−0.1% aqueous TFA (1:1 v/v). The accuracy of mass measurement is regarded as ±0.05%.

PNA Synthesis. NH_2-Cys(NPys)-Lys-CCTCTTACCTCAGTTACA-Lys-amide (PNA705) was synthesized by the Fmoc/Bhoc method using PNA monomers obtained from Link Technologies Ltd. (Lanarkshire, Scotland) on a Liberty microwave peptide synthesizer, purified by HPLC, and characterized by MALDI-TOF mass spectrometry as previously described (*16, 18, 26*).

Conjugation of Peptides to PNA705. Disulfide conjugation between the single Cys residue on the peptide component and the single NPys-Cys residue on the PNA705 was carried out essentially as described previously using a 2.5-fold excess of peptide over PNA705 (*16, 19, 27*). Purification of conjugates by reversed-phase HPLC was carried out using buffers identical to those used for peptide purification and linear gradients, with diode array monitoring at 215 and 260 nm. Products were obtained by lyophilization of desired HPLC fractions. Representative examples of peptide−PNA conjugate crude and puri-

Table 1. List of Branched and Linear Peptides Synthesized and their EC_{50} Values in the RT-PCR Assay in the HeLa pLuc705 Cells

Peptide	Structure	EC50 (μM)
8 Arginines		
RXR4-4B1	R-X-R R-X-R-**K** R-X-R-**K**-**K**-X-β-C R-X-R	> 3
RXR4-4B2	R-X-R-X R-X-R-X-**K** R-X-R-X-**K**-**K**-X-β-C R-X-R-X	> 3
RXR4-4B3	R-X-R R-X-R-**K**-X R-X-R-**K**-X-**K**-X-β-C R-X-R	> 3
RXR4-2B	R-X-R-R-X-R R-X-R-R-X-R-**K**-X-β-C	> 3
RXR4	$(RXR)_4$XC	> 3
12 Arginines		
RXR6-4B	R-X-R-R-X-β R-X-R-R-X-β-**K** R-X-R-R-X-β-**K**-**K**-X-β-C R-X-R-R-X-β	> 3
RXR6-2B	R-X-R-R-X-R-R-X-R R-X-R-R-X-R-R-X-R-**K**-X-β-C	1.3 ± 0.2
RXR6	$(RXR)_6$XβC	1.0 ± 0.1
16 Arginines		
RXR8-4B1	R-X-R-R-X-R R-X-R-R-X-R-**K** R-X-R-R-X-R-**K**-**K**-X-β-C R-X-R-R-X-R	1.2 ± 0.3
RXR8-4B2	R-X-R-R-X-R-X-β R-X-R-R-X-R-X-β-**K** R-X-R-R-X-R-X-β-**K**-**K**-X-β-C R-X-R-R-X-R-X-β	1.3 ± 0.2
RXR8-2B	R-X-R-R-X-R-R-X-R-R-X-R R-X-R-R-X-R-R-X-R-R-X-R-**K**-X-β-C	0.7 ± 0.2
RXR8	$(RXR)_8$XβC	0.8 ± 0.1

fied products are shown in Supporting Information Figure 2. All conjugates were characterized by MALDI-TOF mass spectrometry as described previously (*16, 19, 27*).

Cell Culture and Splicing Redirection Assays. This was carried out similarly to that described previously (*16, 19, 27*). Peptide−PNA conjugates were incubated for 4 h in 0.35 mL OptiMEM medium with exponentially growing HeLa pLuc705 cells (1.25×10^5 cells/well seeded and cultivated overnight in 24 well plates). The medium was removed, 1 mL complete medium (DMEM plus 10% fetal bovine serum) was added, and incubation continued for 20 h. Cells were washed twice with ice-cold PBS and lysed with Reporter Lysis Buffer (Promega, Madison, WI). Luciferase activity was quantified with a Berthold Centro LB 960 luminometer (Berthold Technologies, Bad Wildbad, Germany) using the Luciferase Assay System substrate (Promega, Madison, WI). Cellular protein concentrations were measured with the BCA Protein Assay Kit (Pierce, Rockford, IL) and read using an ELISA plate reader (Dynatech MR 5000, Dynatech Laboratories, Chantilly, VA) at 550 nm. Levels of luciferase expression are shown as relative luminescence units (RLU) per microgram of protein or as fold increase in luminescence over background. All experiments were carried out in triplicate. Each data point was averaged over the three replicates.

For dose-dependence experiments, cells were treated as described above with increasing concentrations of conjugates. After carrying out the luciferase assay and BCA Protein Assay, the remaining cell lysates (about 270 μL) were transferred into 2 mL microfuge tubes, and total RNA was extracted with 1 mL TRI Reagent (Sigma). Minor changes to the manufacturer's protocol were made to accommodate the presence of Reporter Lysis Buffer. Thus, 0.3 mL of chloroform was used for extraction, and the amount of isopropanol for RNA precipitation was increased to give a 1:1 mixture with the aqueous phase. The extracted RNA was examined by RT-PCR (SuperScript III One-Step RT PCR with Platinum Taq, Invitrogen; Genius Techne Thermal cycler) with forward primer 5′-TTG ATA TGT GGA TTT CGA GTC GTC-3′ and reverse primer 5′-TGT CAA TCA GAG TGC TTT TGG CG-3′. The products were analyzed on a 2% agarose gel, which was scanned using *Gene Tools Analysis* Software (SynGene, Cambridge, UK).

Cell Culture and Splicing Redirection Assays at Low Temperature. This was carried out as described previously (*18, 19*). HeLa pLuc705 cells were preincubated for 30 min in OptiMEM at 37 or 4 °C. The conjugate was then added and incubation continued for 1 h before assay for luciferase activity was measured as above.

Cell Culture and Splicing Redirection in the Presence of Endocytosis Inhibitors. This was carried out similarly to the method described previously (*19*). HeLa pLuc705 cells were preincubated in OptiMEM at 37 °C for 20 min with one of the following inhibitors: chlorpromazine (30 μM), methyl-β-cyclodextrin (MBCD) (2.5 mM), nystatin (50 μM), or ammonium chloride (50 mM). Cells were washed twice with PBS and incubated in OptiMEM with the same concentrations of the inhibitors in the presence of 1 μM of peptide−PNA conjugate at 37 °C for 30 min. Cells were washed twice with PBS, 1 mL of DMEM complete medium was added, and incubation continued for 23 h. Each experiment was in triplicate. Luciferase expression was quantified as described above. At these concentrations of inhibitors and under the incubation conditions used, good cell viability was obtained in all cases (data not shown).

RESULTS

Synthesis of PNA705 Conjugates of Linear and Branched (R-Ahx-R)-Containing Peptides. Although the concept of chain branching through α and ε positions of Lys via use of Fmoc Lys(Fmoc)−OH was described first by Futaki (*21*), there were a number of significant differences in our methodology. First, we introduced proteolysis resistant Arg-Ahx-Arg (RXR) units as repeating units instead of oligo-Arg or Arg-$(Gly)_3$-Arg units. Second, we used the proteolysis resistant Ahx-βAla (Xβ) spacer between the branches and the C-terminal Cys residue used for conjugation to cargo, and we also varied the spacing within branches by addition of further X or β units. Third, we investigated 2-branched as well as 4-branched structures. Finally, we attached a PNA cargo via a disulfide bond and used the well-known HeLa pLuc705 cell reporter assay that is a measure of the ability of the peptide dendrimer structure to deliver the

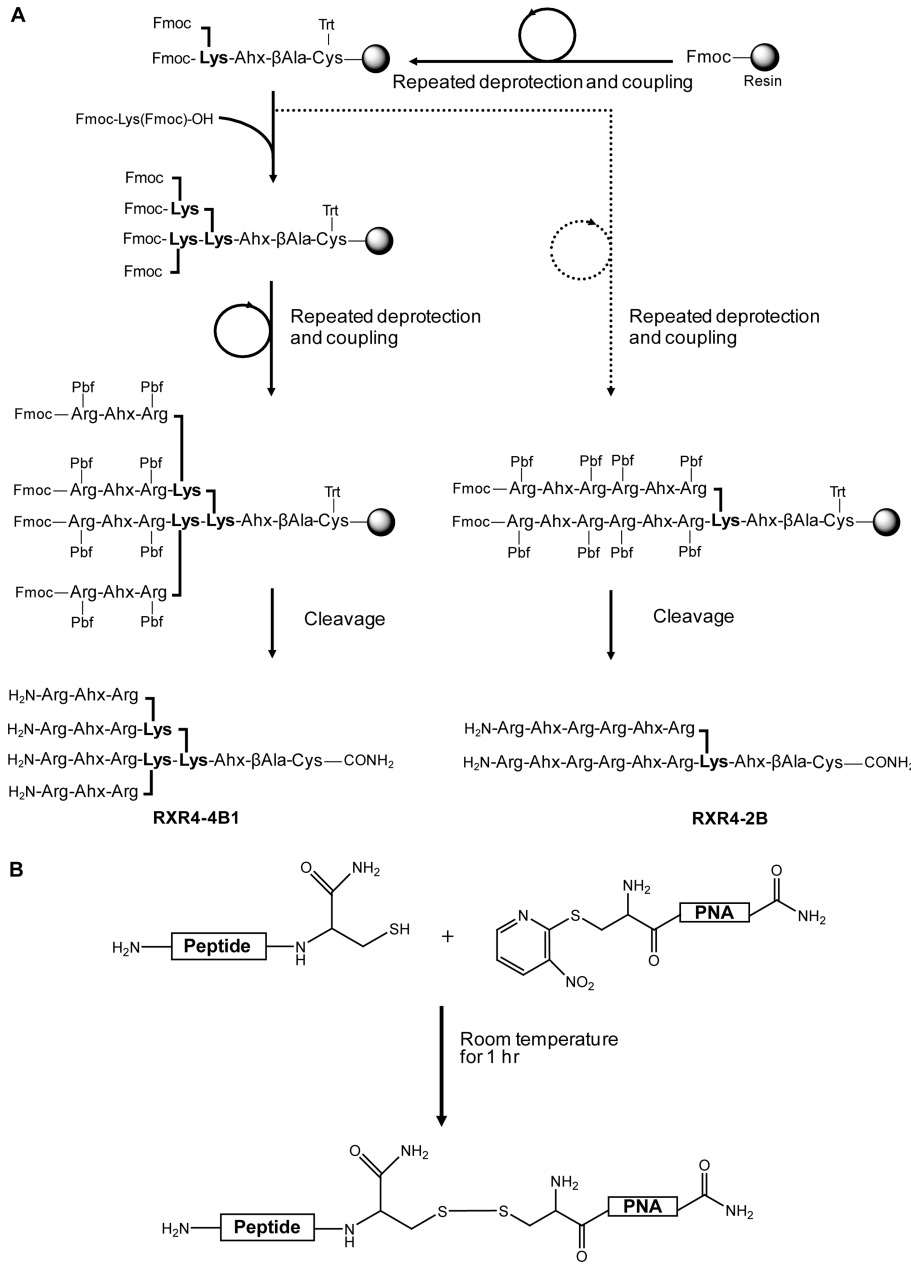

Figure 1. (A) Scheme of solid-phase peptide synthesis of branched peptides RXR4−4B1 and RXR4−2B as representative examples of the strategy of synthesis via branching with Fmoc-Lys (Fmoc)−OH and arms of R-Ahx-R units. Reagents and resin are as described in the Experimental section. (B) Scheme of the disulfide conjugation method used where the PNA contains a NPys-Cys functionality and the peptide a C-terminal free Cys functionality.

cargo to the nucleus. We compared linear (R-Ahx-R) peptides with branched analogues containing the same number of Arg residues, starting with 8-Arg residues $(R\text{-Ahx-R})_4$ and increasing the numbers of Arg residues to 12 and 16. The dendrimer structures and linear peptides RXR4, RXR6 and RXR8 are shown in Table 1.

Synthesis of branched peptide dendrimers (Figure 1A) was carried out very conveniently by microwave-aided solid-phase synthesis using the Fmoc method with a different solid support and different activation agent than reported by Futaki et al. (*21*). The coupling reactions were all very efficient, and only single couplings were needed except for Arg residues. It should be noted that we took account of the need to maintain at least a 5-fold excess of amino acids over solid-support-bound growing chains in coupling reactions at all times by reduction of the amount of solid support for 2- and 4-branched syntheses (see Experimental Procedures). The high yields and efficient syntheses are demonstrated by the HPLC traces obtained for the crude products of synthesis (Supporting Information Figure 1, showing representative 4- and 2-branched dendrimer peptide crude and purified products and MALDI-TOF analysis). Note that it was not necessary to use 5% pyridine/DMF solvent and extended (21 h) coupling times in the FmocArg(Pbf)−OH coupling reactions as previously reported (*21*). Instead, the use of microwave heating and a double coupling protocol proved highly effective (*25*).

Conjugation of purified branched and linear peptides to PNA was carried out through disulfide bond by reaction of each C-terminal Cys-containing peptide with the N-terminal Cys(N-Pys) PNA705 18-mer sequence (Figure 1B) as previously described for other linear cell-penetrating peptides (*16, 18, 19, 27*). Highly efficient conjugations were obtained with only small amounts of unconjugated peptide and PNA remaining (Supporting Information Figure 2 shows representative HPLCs for crude products and purified conjugates for RXR8−4B1-PNA705 and RXR8−2B-PNA705). Note that a disulfide linkage has the

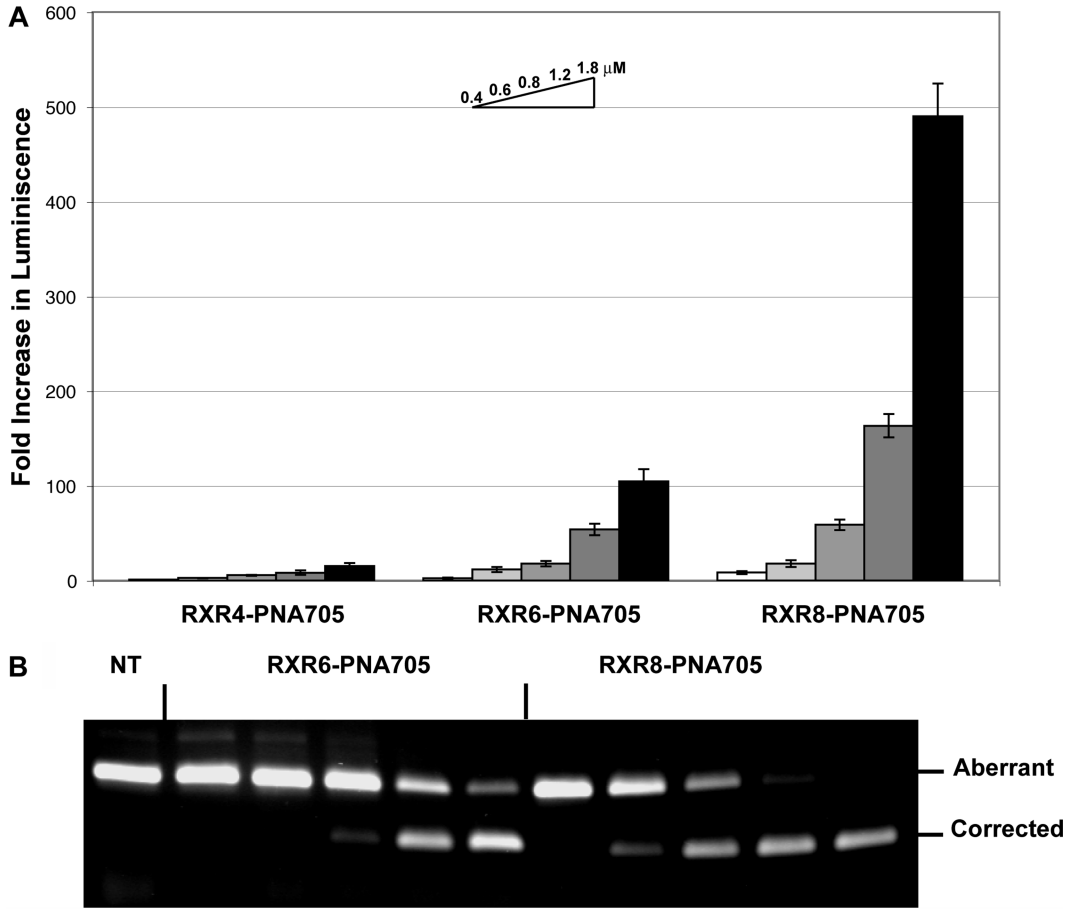

Figure 2. (A) Fold increase in luciferase expression induced by splicing redirection by incubation of RXR4-PNA705, RXR6-PNA705, and RXR8-PNA705 with HeLa pLuc705 cells. Concentrations of conjugates in each case (left to right) are 0.4, 0.6. 0.8. 1.2, and 1.8 μM. (B) RT-PCR analysis showing aberrant and redirected levels of RNA as a function of concentrations of RXR6-PNA705 or RXR8-PNA705. Concentrations of conjugates (left to right) are the same as in (A), namely, 0.4, 0.6, 0.8, 1.2, and 1.8 μM. NT = cells not treated.

advantage that, in principle, the cargo can be released from the peptide vector once inside cells because of the reducing environment, as we have used for our previous R10p53^{tet} dendrimer system (*18*).

Splice-Redirection Activity of Linear and Branched Peptide−PNA Conjugates. We reported previously the splice-redirection activity of linear $(RXR)_4$-PNA and linear $(RXR)_4$-PMO conjugates in the HeLa pLuc705 cell assay (*10, 12*). Although significantly better than $(Lys)_8$, Tat (48−60), Penetratin, and oligoArg conjugates (*12, 19, 28*), EC_{50} values using an RT-PCR assay for the amount of splice-redirected mRNA remained in the micromolar range. To our knowledge, splice-redirection of PNA conjugates to peptide containing a larger number of Arg residues has not been reported previously. We found that for the linear (R-Ahx-R) peptides an increase in the number of Arg residues to 12 (RXR6-PNA705) resulted in a significantly more active conjugate in the luciferase up-regulation assay than RXR4-PNA705, with a further increase in activity for 16 Arg residues (RXR8-PNA705) (Figure 2a). EC_{50} values (Table 1) were determined from the RT-PCR assay by scanning of the agarose gel electrophoregrams (Figure 2b). The biggest improvement in activity was between RXR4 (EC_{50} > 3 μM) and RXR6 (1.0 ± 0.1 μM), whereas a more modest improvement was seen for RXR8 (0.8 ± 0.1 μM).

PNA705 conjugates of 4-branched constructs of RXR4 where each arm contained a single RXR (RXR4−4B1), or a single RXRX (RXR4−4B2), or where additional X spacing was included between the first and second branch points (RXR4−4B3), or a 2-branch analogue with RXRRXR on each branch (RXR4−2B) all showed a dramatic loss of splice-redirecting activity, such that even at 3 μM concentration the luciferase expression activity was barely above background (Figure 3A). Likewise, a 4-branched structure containing four RXRRXβ arms (RXR6−4B) had very poor activity (Figure 3B, Table 1). By contrast, for PNA705 conjugates of RXR6 branched analogues, a 2-branched structure containing arms of RXRRXRRXR (RXR6−2B) gave rise to luciferase expression levels only a little lower than that of the linear RXR6 (Figure 3B, Table 1).

The PNA705 conjugate of RXR8 2-branched analogue (RXR8−2B) showed luciferase expression levels very similar to that for the linear RXR8 (Figure 3C), whereas the 4-branched RXR8 analogues (RXR8−4B1 and RXR8−4B2) were only slightly reduced in activity compared to the linear RXR8 (Figure 3C). The EC_{50} values (Table 1) for splice-redirected RNA measured by the RT-PCR assay in general reflected the same trends as for luciferase up-regulation results, with values for PNA705 conjugates of 2-branched peptides with 12 and 16 residues being very similar to their linear counterparts. Overall, chain branching appears to be best tolerated when the number of Arg residues is 16. For both 12 and 16 Arg residues, 2-branched structures are more active than 4-branched structures and are similar to their linear counterparts in activity. None of the 12 and 16 Arg residue conjugates showed significant toxicity, and the cell viability remained good in an MTS assay up to 3 μM with HeLa pLuc705 cells (Figure 4).

We also carried out the same luciferase and RT-PCR assays for RXR8−4B-PNA705, RXR8−2B-PNA705, and RXR8-PNA705 using a human melanoma tumor cell line containing the same integrated pLuc705 plasmid, namely, A375SM-Luc705-B cells (*29*). The results were broadly similar to the

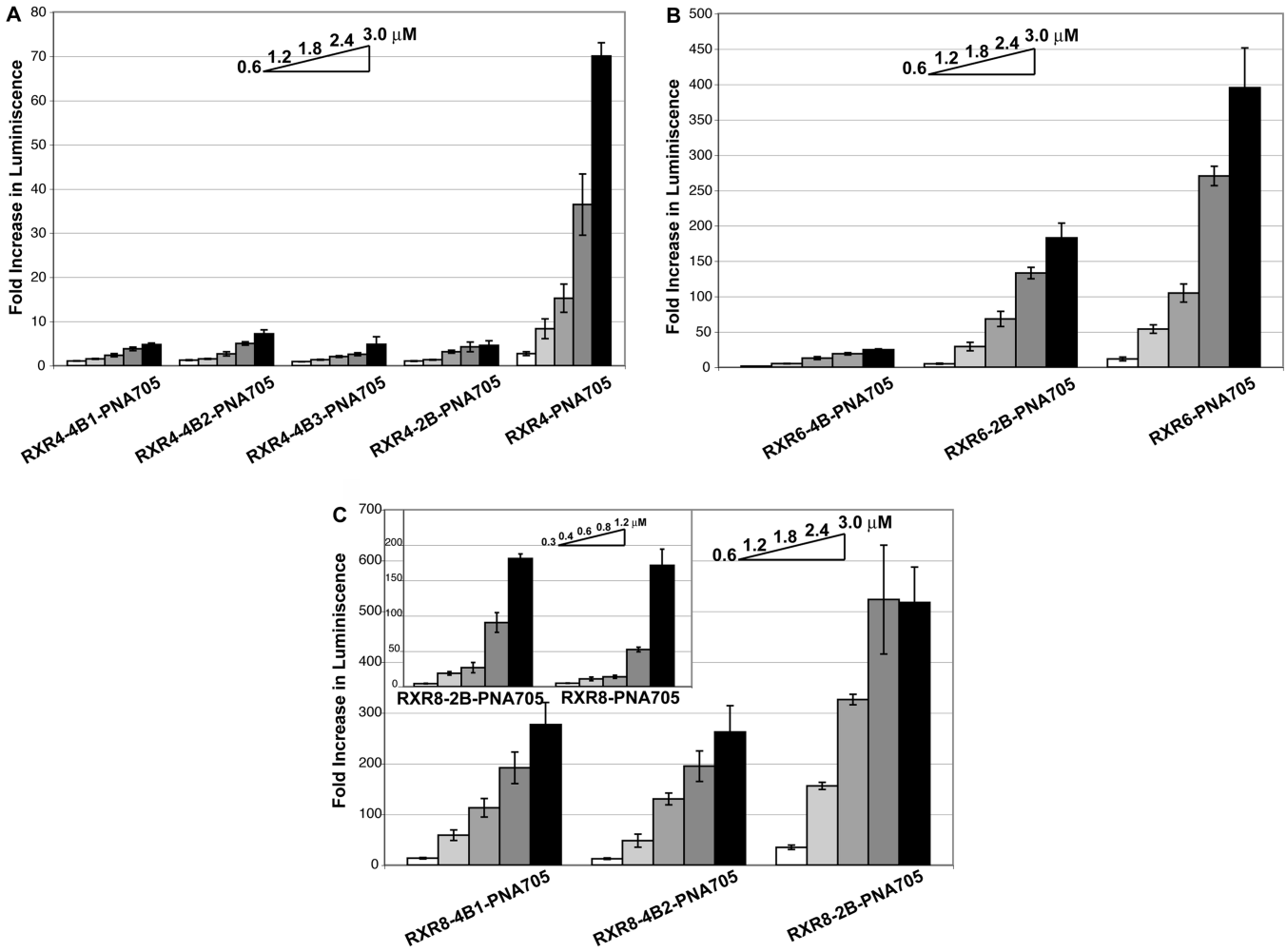

Figure 3. Fold increase in luciferase expression induced by splicing redirection in HeLa pLuc705 cells over the conjugate concentration range 0.6−3.0 μM: (A) branched and linear RXR4-PNA705 derivatives, (B) branched and linear RXR6-PNA705 derivatives, and (C) branched RXR8-PNA705 derivatives (inset shows a comparison of RXR8-2B-PNA705 and linear RXR8-PNA705 over a different concentration range 0.3−1.2 μM).

HeLa cell results in splice-redirecting activity, but in each case, the EC_{50} values in the RT-PCR assay were lower than for the HeLa cells (RXR8−4B1, 0.51 ± 0.03 μM; RXR8−2B, 0.35 ± 0.02 μM; RXR8, 0.42 ± 0.05 μM), probably reflecting a lower copy number of integrated pLuc705 plasmid in the melanoma cell line, but cell viability dropped significantly at 1 μM and higher concentrations for all these peptide−PNA conjugates (data not shown).

In addition, we carried out the HeLa pLuc705 cell luciferase assays at 1.2 μM concentration for 4 h in the presence of 10% fetal bovine serum (FBS). Interestingly, in most cases for 12 Arg and 16 Arg conjugates of PNA705 there was significant activity retained in the presence of serum, compared to serum-free media, especially for the 2-branched and the linear constructs (Supporting Information Figure 3). This is in contrast to unbranched peptide−PNA conjugates containing fewer Arg residues such as RXR4-PNA and R6Pen-PNA, where we had previously found very poor activity in the presence of serum (Arzumanov, A., Abes, R., Gait, M. J., and Lebleu, B., unpublished data).

Thus, we also synthesized a 25-mer PMO conjugate of RXR8−2B targeted to exon 23 of a mutated mouse dystrophin gene by the method previously described (*16*). At 1 μM concentration of incubation with differentiated *mdx* mouse cells in the presence of 10% FBS, but in the absence of any transfection agent, we were able to obtain >70% exon skipping in this model system, higher than for previously studied linear RXR peptide−PMO constructs (data not shown). This demonstrates that there are potential advantages of a higher number of Arg residues in the peptides in terms of activity levels in the presence of serum, which could be crucial for clinical applications.

Mechanism of Cell Uptake in HeLa pLuc705 Cells. The internalization mechanism of CPPs has been questioned ever since the first peptides were discovered. Initially, the consensus in the field was for direct translocation across the plasma membrane, but nowadays, endocytosis is considered the major pathway for many CPPs at low concentrations (*2*). We thus felt it necessary to determine whether increased biological activity of our branched peptide conjugates in comparison with the linear forms could be due to the use of a different cell uptake route. We first examined the splicing redirection activity of these peptide conjugates at low temperature of 4 °C (conditions preventing any form of endocytosis) and physiological temperature 37 °C. Cells were preincubated at 4 or 37 °C during 30 min and then incubated with the different branched peptide conjugates at 1 μM during 1 h at 4 or 37 °C. The results showed a decrease of the activity at low temperature, suggesting that the internalization of the branched peptide conjugates is predominantly energy dependent (Figure 5).

Likewise, controversies remain concerning the endocytotic pathway used for the cell internalization pathway of CPP−cargo conjugates with data advocating all three major routes (*2, 3*). We thus investigated the effects of typical inhibitors of clathrin-dependent, caveolae-dependent, and macropinocytosis pathways,

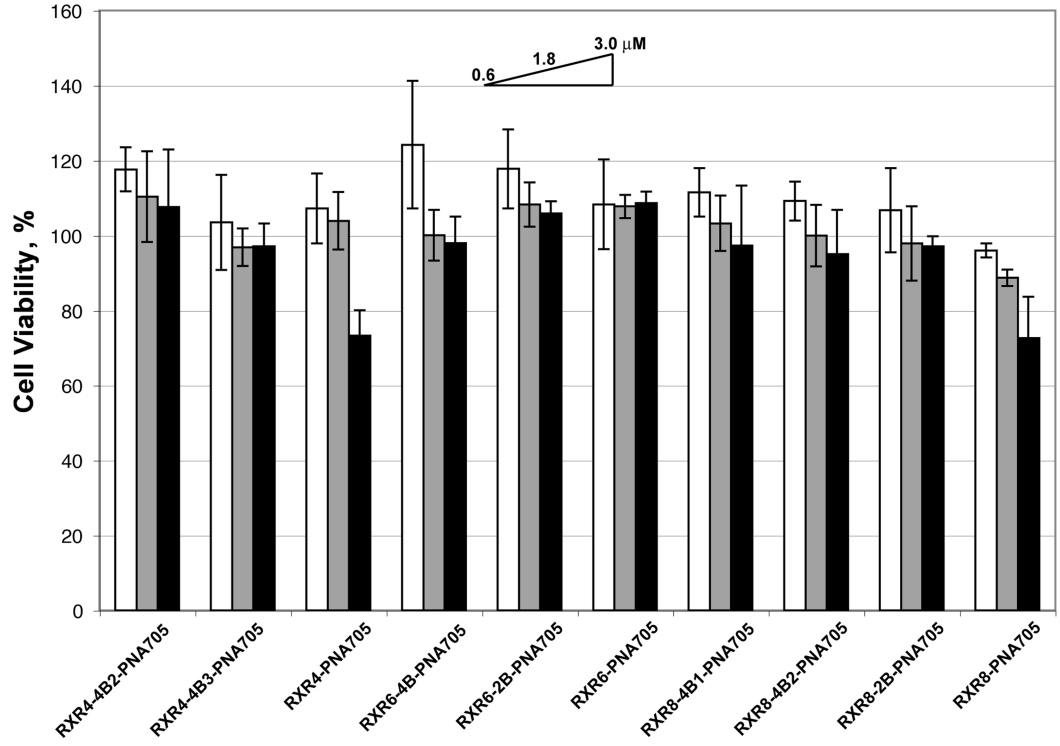

Figure 4. Percentage cell viability for branched and linear peptide-PNA705 conjugates as measured by the MTS assay. To each well of cells treated for 4 h with 0.6, 1.8, or 3.0 μM conjugate in OptiMEM (100 μL, 96 well plate) was added 20 μL of CellTiter 96 Aqueous One solution cell proliferation assay (Promega) and the color intensity measured by plate reader (Tecan, Switzerland) at 490 nm as compared to a control of cells which were not treated with conjugate. Experiments were carried out in triplicate.

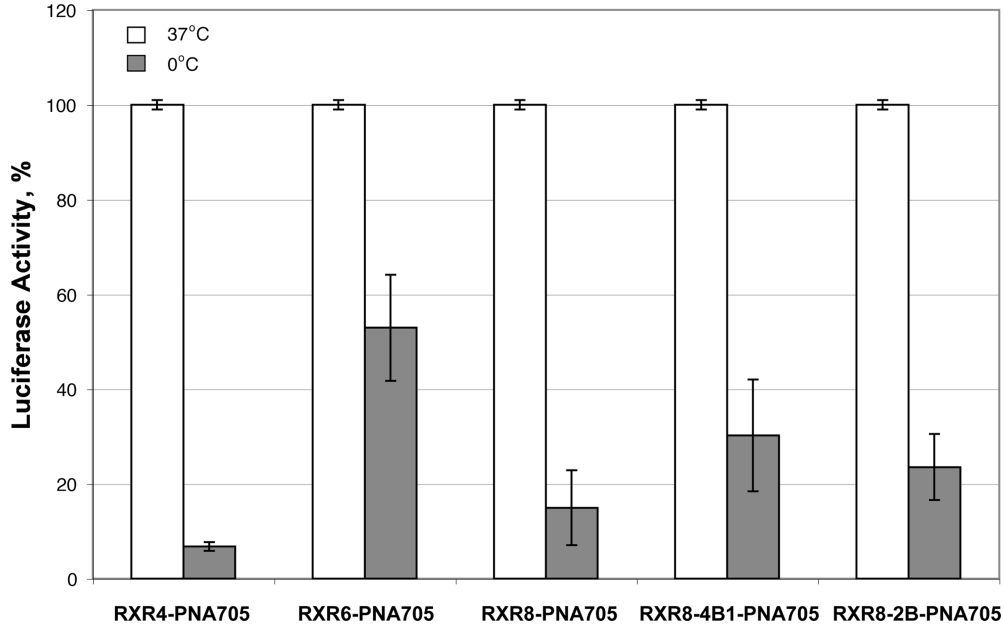

Figure 5. Low-temperature study (37 and 4 °C). Cells were preincubated at 37 °C (white bars) or 4 °C (gray bars) for 1 h and further incubated in the same conditions with PNA705 conjugates of RXR4, RXR6, RXR8, RXR8−4B1, or RXR8−2B, peptides conjugates at 1 μM. Luciferase expression assays were carried out after 24 h as indicated in the Experimental Procedures. Experiments were made in triplicate, and error bars are indicated. Data are expressed as the percentage of luciferase activity.

which are chlorpromazine, nystatin, and methyl-β-cyclodextrin (MBCD), respectively. The importance of acidification of endocytotic vesicles was evaluated with NH_4Cl. For these experiments, incubation times were reduced in order to avoid cytotoxicity of the inhibitors. Interestingly, splicing redirection efficiency by branched CPPs remained unchanged when reducing the incubation time to 30 min as compared to the 4 h incubations generally used in our studies. This is very different from the situation observed with RXR4-PMO conjugate, for example (data not shown).

Nystatin addition resulted in some reduction in the biological activity of both linear and branched peptides (Figure 6). Since nystatin complexes cholesterol and alters the structure and function of glycolipid microdomains, caveolae seem to be involved. Somewhat surprisingly, the activity increased using methyl-β-cyclodextrin, suggesting that branched peptides may

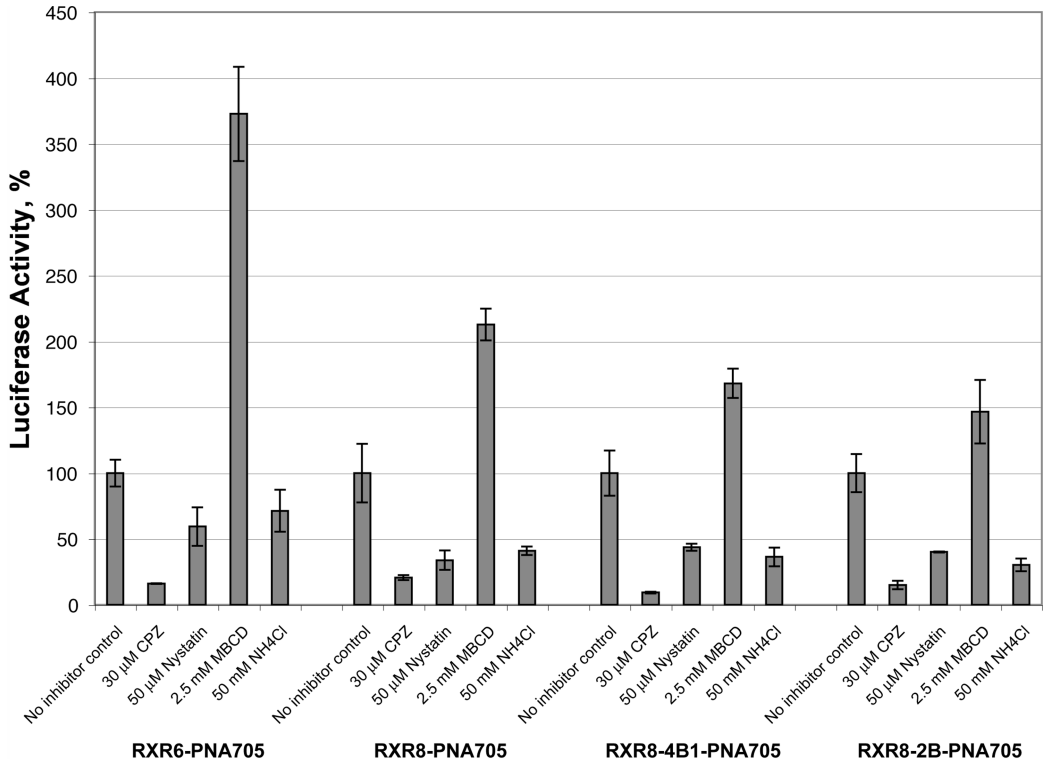

Figure 6. Luciferase activity of PNA705 conjugates of RXR6, RXR8, RXR8−4B1, or RXR8−2B using endocytosis inhibitors. Cells were preincubated at 37 °C for 20 min with chlorpromazine (30 μM), methyl-β-cyclodextrin (MBCD) (2.5 mM), nystatin (50 μM), or ammonium chloride (50 mM). Cells were further incubated in the same conditions with the peptide conjugates at 1 μM for 30 min. Luciferase expression assays were carried out after 24 h as indicated in the Experimental Procedures. Experiments were made in triplicate, and error bars are indicated. Data are expressed as the percentage of luciferase activity.

become internalized by direct membrane translocation into the cytoplasm when the membrane cholesterol is depleted, as previously reported for oligoArg (*30*). By contrast, chlorpromazine exerted a very strong effect on the biological activity with almost 90% decrease for RXR8−2B-PNA and RXR8−4B1-PNA (Figure 6). Together, these data support the notion that the clathrin-dependent uptake pathway is prominently and preferentially involved in the internalization of the branched peptides, as has already been documented for linear RXR4-PMO (*11*), Pip peptide−PNA conjugates (*16*), and Tat peptide (*15*), but with some caveolae dependence also.

Cells were also treated with NH_4Cl, which is known to neutralize the acidification of endosomal and lysosomal compartments (*31*). NH_4Cl (50 mM) caused a strong reduction in the splicing redirection activity of both linear and branched peptides with 16 Arg residues suggesting there is an accumulation in acidic compartment as shown previously for Tat−PNA conjugates (*15*) and a requirement for endosomal acidification for endosomal escape (Figure 6).

DISCUSSION

Synthesis of branched dendrimer peptides using R-Ahx-R repeating units proved very straightforward by the use of microwave-aided Fmoc solid-phase synthesis techniques. Indeed, the number of coupling steps in branched peptide syntheses is less than that for the equivalent linear peptide syntheses containing the same number of Arg residues, and the HPLC traces of the crude products all showed very high overall yields (Supporting Information Figure 1). Disulfide conjugations to PNA were just as effective as for linear peptides (Supporting Information Figure 2).

The use of a HeLa pLuc705 splice-redirecting assay for assessment of CPPs is particularly valuable to judge delivery efficacy because of its convenience, large dynamic range and its ability to measure activity in the cell nucleus for attached PNA or PMO through assays at both the RNA and protein expression levels. In our opinion, a functional assay of this type is superior to the use of fluorescent labels and observation of cell localization by confocal microscopy, because it is a true measure of the ability of a cargo to be delivered in a biologically relevant way, in this case to the cell nucleus. Thus, despite the apparently promising results of Futaki et al. for a 4-branched RG_3R peptide with 8-Arg residues in total where substantial cell uptake of the peptide was observed when a fluorescent label was attached (*21, 22*), by contrast, we found extremely poor luciferase up-regulation in the HeLa cell assay for PNA705 conjugates of both 2-branched and 4-branched peptide with only 8 Arg residues and much poorer than the linear RXR4-PNA. This suggests that branching the 8 Arg residues in this way does not trigger sufficient endosomal escape of the PNA cargo and represents a good example of how following the uptake of fluorescently labeled peptides by confocal microscopy is not predictive of subsequent biological function. We already observed a lack of correlation between cell uptake and biological activity in our SAR studies of a series of linear RXR−PMO conjugates (*13*).

As the number of Arg residues is increased to 12 and 16, however, not only does the overall level of luciferase up-regulation and splicing correction increase significantly with the number of Arg residues, but chain branching is now increasingly tolerated (Figures 2 and 3). An increase in splice-redirecting activity as the number of Arg residues is raised from 8 to 12 and 16 is not surprising, since the overall cell uptake for oligo-Arg peptides of 5 to 8 residues was shown to increase as a function of the number of Arg residues (*32*). However, the number of Arg residues and the precise three-dimensional configuration within the peptide may also affect other steps in the delivery to the nucleus. In general, we found that the longer

the run of R-Ahx-R motifs on each arm, the better the activity for the same total number of Arg residues. In the linear (R-Ahx-R)$_4$ peptide, we found previously that aminohexanoic acid spacing between guanidinium groups was optimal for splice-redirecting activity for an attached PMO oligonucleotide compared to shorter or longer spacers (*13*). Further work will be necessary to understand if this finding also holds true for the branched peptides.

However, a differential level of overall cell uptake by linear and branched peptides cannot be ruled out, especially since it has been shown for fluorescently labeled branched 8-Arg peptides that they are more dependent on interaction with membrane-associated heparan sulfate proteoglycans on the cell surface compared to linear R_8 peptides (*22*). Nevertheless, our data are consistent with the notion that the active fraction of branched Arg-rich peptide−PNAs does not use a different pathway of uptake compared to the linear R-Ahx-R peptides. This is evidenced by the very similar deleterious effects on luciferase up-regulation activity seen upon lowering the temperature of the splice correction assay to 4 °C and the similar behavior upon coincubation with endocytosis inhibitors for both branched and linear peptide−PNA constructs (Figures 5 and 6).

The very large effect of chlorpromazine on 16-Arg branched and linear peptide−PNA conjugates (Figure 6) was similar to the effects we previously observed in the same HeLa pLuc705 cells for other highly cationic peptide conjugates of PNA and PMO, such as linear RXR4-PMO (*11*), Pip peptide-PNA (*16*), and Tat peptide (*15*). We conclude as before that clathrin-dependent uptake predominates. However, the effect of nystatin on the luciferase up-regulation was much larger in the cases of both linear and branched RXR−PNA conjugates compared to the only small effects observed of nystatin on uptake and activity of the Tat peptide (*15*) and on Pip-PNA (*16*). This surprising result suggests that caveolae may play some part in uptake where there are a larger number of Arg residues, as has already been shown for Tat fusion proteins (*33*). This could account for the moderate effect of NH_4Cl in some cases, since caveolae-mediated endocytosis does not involve acidic compartments (*34*).

Our results are not entirely consistent with inhibitor experiments in the same cell assay for PNA705 conjugates of moderately cationic, Arg-containing peptides Penetratin and M918, where macropinocystosis was suggested as the major uptake pathway and clathrin-dependent endocytosis predominated only for the more hydrophobic TP10-PNA conjugate (*35*). The concentration of chlorpromazine used in our case was 30 μM, whereas in the case of Lundin et al., it was only 10 μM, and the peptide−PNA concentrations used in our case were 5-fold lower. Poon et al. reported for R_8-functionalized liposome uptake that endocytotic uptake switches from clathrin-dependent to macropinocytosis as peptide density on the liposome surface was increased (*36*), and a mechanism switch is one possible explanation for the discrepancy between our studies and those of Lundin et al. Another possibility is that the choice of uptake pathway is more subtly affected by the different relative positions of the hydrophobic and cationic elements in M918 and Penetratin as compared to the R-Ahx-R constructs. The possible sensitivity of inhibitor use to different cellular conditions, as well as possible subtle effects of amino acid composition and positioning, makes it hard to draw too definitive conclusions about the endocytosis pathways used by cationic CPPs in this class when conjugated to PNA. Further, our result that MBCD addition significantly stimulated luciferase up-regulation suggests that, when one pathway is inhibited, it is possible for cells to utilize or stimulate an alternative uptake pathway. More sophisticated cell techniques will be needed to clarify the dominant endocytotic uptake pathways for particular peptide−cargo conjugates.

A major aim of our experiments was to determine whether branched R-Ahx-R peptides could prove suitable for future development in a therapeutic context. We were particularly heartened that significant splice-redirecting activity was retained in the HeLa cell assay in the presence of 10% serum for many of the 12-Arg and 16-Arg containing conjugates (Supporting Information Figure 3), and we obtained extremely high exon skipping for RXR8−2B-PMO in a *mdx* mouse muscle cell assay that is used as a model for DMD (data not shown). However, we became concerned about the possibility of increased toxicity resulting from the use of larger numbers of Arg residues in the peptides. Although we did not observe toxicity up to 3 μM in the HeLa pLuc705 cell assay (Figure 4), we did see significant loss of cell viability at 1 μM in A375SM-Luc705-B melanoma cells for all 12 and 16 Arg conjugates (data not shown). Further, a very recent report has suggested that at high doses in both mice and monkeys some kidney toxicity is apparent when an 8-Arg peptide-PMO is injected intravenously (*6*). Thus, despite the substantial increase in cell delivery potential afforded by such dendrimeric peptide constructs, peptide conjugates with high Arg content must be used with caution in therapeutic development until the sources of these toxicities (both cellular and in vivo) can be controlled. In the case of cells, more detailed studies of membrane leakage or other specific cell toxicity assays could prove instructive.

Nevertheless, our studies have been useful in understanding some of the three-dimensional requirements for cell uptake and splice-redirecting activity of Arg-rich peptides based on an R-Ahx-R motif, and we have demonstrated that chain branching is well-tolerated when the number of Arg residues is high, especially for 2-branched peptide structures. We have shown also how such peptide chain branching is readily accessible chemically and in high yield. In principle, our methods could be used also to introduce other multiple motifs such as cell-specific uptake sequences (*17*) as conjugates of PNA or PMO cargoes. Our work expands the three-dimensional space available for CPP development.

ACKNOWLEDGMENT

We thank Rudy Juliano (University of North Carolina) for the cell line A375SM pLuc705-B. Amer Saleh was supported in part by a grant from MRC-Technology and Rachida Abes by a PhD fellowship from the Ligue Nationale contre le Cancer. We thank Donna Williams for chemical synthesis of PNA705.

Supporting Information Available: HPLC purifications of representative synthesis of branched peptides and peptide-PNA conjugates, and luciferase up-regulation results for 16-Arg constructs in HeLa pLuc705 cells in the presence of 10% FBS. This material is available free of charge via the Internet at http://pubs.acs.org.

LITERATURE CITED

(1) Langel, U. (2007) *Handbook of Cell Penetrating Peptides*, p 600, CRC Press, Boca Raton.

(2) Lebleu, B., Moulton, H. M., Abes, R., Ivanova, G. D., Abes, S., Stein, D. A., Iversen, P. L., Arzumanov, A., and Gait, M. J. (2008) Cell penetrating peptide conjugates of steric block oligonucleotides. *Adv. Drug Delivery Rev. 60*, 517–529.

(3) Said Hassane, F., Saleh, A. F., Abes, R., Gait, M. J., and Lebleu, B. (2010) Cell penetrating peptides: overview and applications to the delivery of oligonucleotides. *Cell. Mol. Life Sci. 67*, 715–726.

(4) Fabani, M. M., Ivanova, G. D., and Gait, M. J. (2008) Peptide-peptide nucleic acid conjugates for modulation of gene expres-

sion, in *Therapeutic Oligonucleotides* (Kurreck, J., Ed.) pp 80−102, Royal Society of Chemistry, Cambridge, U.K.
(5) Moulton, H. M., and Moulton, J. D. (2008) Antisense morpholino oligomers and their peptide conjugatesin, in *Therapeutic Oligonucleotides* (Kurreck, J., Ed.) pp 43−79, Royal Society of Chemistry, Cambridge, U.K.
(6) Moulton, H. M., and Moulton, J. D. (2010) Morpholinos and their peptide conjugates: therapeutic promise and challenge for Duchenne muscular dystrophy. *Biochim. Biophys. Acta*, doi: 10.1016/j.bbamem.2010.02.012.
(7) Wood, M. J. A. (2010) Towards an oligonucleotide therapy for Duchenne muscular dystrophy: a complex development challenge. *Sci. Translat. Med. 2*, 25ps15.
(8) Richard, J.-P., Melikov, K., Vivès, E., Ramos, C., Verbeure, B., Gait, M. J., Chernomordik, L. V., and Lebleu, B. (2003) Cell-penetrating peptides. A re-evaluation of the mechanism of cellular uptake. *J. Biol. Chem. 278*, 585–590.
(9) Kang, S.-H., Cho, M.-J., and Kole, R. (1998) Up-regulation of luciferase gene expression with antisense oligonucleotides: implications and applications in functional assay development. *Biochemistry 37*, 6235–6239.
(10) Abes, R., Arzumanov, A., Moulton, H. M., Abes, S., Ivanova, G. D., Iversen, P. L., Gait, M. J., and Lebleu, B. (2007) Cell-penetrating-peptide-based delivery of oligonucleotides: an overview. *Biochem. Soc. Trans. 35*, 775–779.
(11) Abes, S., Moulton, H. M., Clair, P., Prevot, P., Youngblood, D. S., Wu, R. P., Iversen, P. L., and Lebleu, B. (2006) Vectorization of morpholino oligomers by the (R-Ahx-R)$_4$ peptide allows efficient splicing correction in the absence of endosomolytic agents. *J. Controlled Release 116*, 304–313.
(12) Abes, S., Moulton, H. M., Turner, J. J., Clair, P., Richard, J.-P., Iversen, P. L., Gait, M. J., and Lebleu, B. (2007) Peptide-based delivery of nucleic acids: design, mechanism of uptake and applications to splice-correcting oligonucleotides. *Biochem. Soc. Trans. 35*, 53–55.
(13) Abes, R., Moulton, H. M., Clair, P., Yang, S. T., Abes, S., Melikov, K., Prevot, P., Youngblood, D. S., Iversen, P. L., Chernomordik, L. V., and Lebleu, B. (2008) Delivery of steric block morpholono oligomers by (R-X-R)4 peptides: structure-activity studies. *Nucleic Acids Res. 36*, 6343–6354.
(14) Wender, P. A., Mitchell, D. J., Pattabiraman, K., Pelkey, E. T., Steinman, L., and Rothbard, J. B. (2000) The design, synthesis, and evaluation of molecules that enable or enhance cellular uptake: peptoid molecular transporter. *Proc. Natl. Acad. Sci. U.S.A. 97*, 13003–13008.
(15) Richard, J. P., Melikov, K., Brooks, H., Prevot, P., Lebleu, B., and Chernomordik, L. V. (2005) Cellular uptake of unconjugated TAT peptide involves clathrin-dependent endocytosis and heparan sulfate receptors. *J. Biol. Chem. 280*, 15300–15306.
(16) Ivanova, G. D., Arzumanov, A., Abes, R., Yin, H., Wood, M. J. A., Lebleu, B., and Gait, M. J. (2008) Improved cell-penetrating peptide-PNA conjugates for splicing redirection in HeLa cells and exon skipping in *mdx* mouse muscle. *Nucleic Acids Res. 36*, 6418–6428.
(17) Yin, H., Moulton, H. M., Betts, C., Seow, Y., Boutilier, J., Iversen, P. L., and Wood, M. J. A. (2009) A fusion peptide directs enhanced systemic dystrophin exon skipping and functional restoration in dystrophin-deficient *mdx* mice. *Hum. Mol. Genet. 18*, 4405–4414.
(18) Said Hassane, F., Ivanova, G. D., Bolewska-Pedyczak, E., Abes, R., Arzumanov, A., Gait, M. J., Lebleu, B., and Gariépy, J. (2009) A peptide-based dendrimer that enhances the splice-redirecting activity of PNA conjugates in cells. *Bioconjugate Chem. 20*, 1523–1530.
(19) Abes, S., Turner, J. J., Ivanova, G. D., Owen, D., Williams, D., Arzumanov, A., Clair, P., Gait, M. J., and Lebleu, B. (2007) Efficient splicing correction by PNA conjugation to an R_6-Penetratin delivery peptide. *Nucleic Acids Res. 35*, 4495–4502.
(20) Kawamura, K. S., Sung, M., Bolewska-Pedyczak, E., and Gariépy, J. (2006) Probing the impact of valency on the routing of arginine-rich peptides into eukaryotic cells. *Biochemistry 45*, 1116–1127.
(21) Futaki, S., Nakase, I., Suzuki, T., Youjun, Z., and Sugiura, Y. (2002) Translocation of branched-chain arginine peptides through cell membranes: flexibility in the spacial disposition of positive charges in membrane-permeable peptides. *Biochemistry 41*, 7925–7930.
(22) Nakase, I., Tadokoro, A., Kawabata, N., Takeuchi, T., Katoh, H., Hiramoto, K., Negishi, M., Nomizu, M., Sugiura, Y., and Futaki, S. (2007) Interaction of arginine-rich peptides with membrane-associated proteoglycans is crucial for induction of actin organization and macropinocytosis. *Biochemistry 46*, 492–501.
(23) Li, Y.-F., and Morcos, P. A. (2008) Design and synthesis of dendritic molecular transporter that achieves efficient *in vivo* delivery of morpholino antisense oligo. *Bioconjugate Chem. 19*, 1464–1470.
(24) Wu, B., Li, Y.-F., Morcos, P. A., Doran, T. J., Lu, P., and Lu, Q. L. (2009) Octa-guanidine morpholino restores dystrophin expression in cardiac and skeletal muscles and ameliorates pathology in dystrophic mdx mice. *Mol. Ther. 17*, 864–871.
(25) Banerjee, J., Hanson, A. J., Muhonen, W. W., Shabb, J. B., and Mallik, S. (2010) Microwave-assisted synthesis of triple-helical collagen-mimetic lipopeptides. *Nat. Protoc. 5*, 39–50.
(26) Fabani, M. M., Abreu-Goodger, C., Williams, D., Lyons, P. A., Torres, A., Smith, K. G. C., Enright, A. J., Gait, M. J., and Vigorito, E. (2010) Efficient inhibition of miR-155 function in vivo by Peptide Nucleic Acids. *Nucleic Acids Res. 38*, 4466–4475.
(27) Turner, J. J., Ivanova, G. D., Verbeure, B., Williams, D., Arzumanov, A., Abes, S., Lebleu, B., and Gait, M. J. (2005) Cell-penetrating peptide conjugates of peptide nucleic acids (PNA) as inhibitors of HIV-1 Tat-dependent trans-activation in cells. *Nucleic Acids Res. 33*, 6837–6849.
(28) Abes, S., Williams, D., Prevot, P., Thierry, A. R., Gait, M. J., and Lebleu, B. (2006) Endosome trapping limits the efficiency of splicing correction by PNA-oligolysine conjugates. *J. Controlled Release 110*, 595–604.
(29) Alam, M. R., Dixit, V., Kang, H., Li, Z.-B., Chen, X., Trejo, J., Fisher, M., and Juliano, R. L. (2008) Intracellular delivery of an anionic antisense oligonucleotide via receptor mediated endocystosis. *Nucleic Acids Res. 36*, 2764–2776.
(30) Futaki, S., Nakase, I., Tadokoro, A., Takeuchi, T., and Jones, A. T. (2007) Arginine-rich peptides and their internalization mechanisms. *Biochem. Soc. Trans. 35*, 784–787.
(31) Zhang, X., Jin, Y., Plummer, M. R., Pooyan, S., Gunaseelan, S., and Sinko, P. J. (2009) Endocytosis and membrane potential are required for HeLa cell uptake of R.I.-CKTat9, a retro-inverso Tat cell penetrating peptide. *Mol. Pharmaceutics 6*, 836–848.
(32) Goun, E. A., Pillow, T. H., Jones, L. R., Rothbard, J. B., and Wender, P. A. (2006) Molecular transporters: synthesis of oligoguanidinium transporters and theor application to drug delivery and real-time imaging. *ChemBioChem 7*, 1497–1515.
(33) Ferrari, A., Pellegrini, V., Arcangeli, C., Fittipaldi, A., Giacci, M., and Beltram, F. (2003) Caveolae-mediated internalization of extracellular HIV-1 Tat fusion proteins visualized in real time. *Mol. Ther. 8*, 284–294.
(34) Pelkmans, L., Kartenbeck, J., and Helenius, A. (2001) Caveolar endocytosis of simian virus 40 reveals a new two-step vesicular transport pathway to the ER. *Nat. Cell Biol. 3*, 473–483.
(35) Lundin, P., Johansson, H., Guterstam, P., Holm, T., Hansen, M., Langel, U., and El-Andalousi, S. (2008) Distinct uptake routes of cell-penetrating peptide conjugates. *Bioconjugate Chem. 19*, 2535–2542.
(36) Poon, G. M. K., and Gariépy, J. (2007) Cell-surface proteoglycans as molecular portals for cationic peptide and polymer emtry into cells. *Biochem. Soc. Trans. 35*, 788–793.

BC100275R